Elucidation of the Charging Mechanisms and the Coupled Structural–Mechanical Behavior of Ti₃C₂Tₓ (MXenes) Electrodes by In Situ Techniques

$\text{Ti}_3\text{C}_2\text{T}_x$

Bergman, Gil; Ballas, Elad; Gao, Qiang; Nimkar, Amey; Gavriel, Bar; Levi, Mikhael D.; Sharon, Daniel; Malchik, Fyodor; Wang, Xuehang; More Authors

Citation (APA)
Bergman, G., Ballas, E., Gao, Q., Nimkar, A., Gavriel, B., Levi, M. D., Sharon, D., Malchik, F., Wang, X., & More Authors (2023). Elucidation of the Charging Mechanisms and the Coupled Structural–Mechanical Behavior of Ti₃C₂Tₓ (MXenes) Electrodes by In Situ Techniques. *Advanced Energy Materials*, *13*(8), Article 2203154. https://doi.org/10.1002/aenm.202203154

Important note
To cite this publication, please use the final published version (if applicable).
Please check the document version above.

Elucidation of the Charging Mechanisms and the Coupled Structural–Mechanical Behavior of Ti$_3$C$_2$T$_x$ (MXenes) Electrodes by In Situ Techniques

Gil Bergman, Elad Ballas, Qiang Gao, Amey Nimkar, Bar Gavriel, Mikhael D. Levi, Daniel Sharon, Fyodor Malchik,* Xuehang Wang,* Netanel Shpigel,* Daniel Mandler, and Doron Aurbach*

The discovery of the Ti$_3$C$_2$T$_x$ compounds (MXenes) a decade ago opened new research directions and valuable opportunities for high-rate energy storage applications. The unique ability of the MXenes to host various mono- and multivalent cations and their high stability in different electrolyte environments including aqueous, organic, and ionic liquid solutions, promoted the rapid development of advanced MXene-based electrodes for a large variety of applications. Unlike the vast majority of typical intercalation compounds, the electrochemical performance of MXene electrodes is strongly influenced by the presence of co-inserted solvent molecules, which cannot be detected by conventional current/potential electrochemical measurements. Furthermore, the electrochemical insertion of ions into MXene interspaces results in strong coupling with the intercalation-induced structural, dimensional, and viscoelastic changes in the polarized MXene electrodes. To shed light on the charging mechanisms of MXene systems and their associated phenomena, the use of a large variety of real-time monitoring techniques has been proposed in recent years. This review summarizes the most essential findings related to the charging mechanism of Ti$_3$C$_2$T$_x$ electrodes and their potential induced structural and mechanical phenomena obtained by in situ investigations.

1. Introduction

The need for improved highly efficient electrochemical systems enabling high power and energy densities, as well as long-time operation stability, provides a tremendous impetus to the development of new classes of electrode materials for batteries and supercapacitors applications. Over the last decades, novel electrode materials, possessing capacitive and pseudocapacitive properties, combining both batteries (faradaic) and supercapacitors (non-faradaic) features have conceptually enriched the broad field of materials science for energy storage and conversion.[1] Special efforts have been devoted to the development of new compounds for beyond-Li batteries applications, enabling reversible storage of various mono- and multivalent ions such as Na$^+$, K$^+$, Mg^{2+}, Ca^{2+}, and Zn^{2+}.[2] In this regard, one of the promising families of electrodes materials

G. Bergman, E. Ballas, A. Nimkar, B. Gavriel, M. D. Levi, D. Aurbach
Department of Chemistry
BINA–BIU Center for Nanotechnology and Advanced Materials
Bar-Ilan University
Ramat-Gan 5290002, Israel
E-mail: Doron.Aurbach@biu.ac.il
Q. Gao
Scanning Probe Microscopy Group
Center for Nanophase Materials Sciences
Oak Ridge National Laboratory
Oak Ridge, TN 37831, USA

The ORCID identification number(s) for the author(s) of this article can be found under https://doi.org/10.1002/aenm.202203154.

Q. Gao
Owens Corning Science & Technology
Granville, OH 43023, USA
D. Sharon, N. Shpigel, D. Mandler
Institute of Chemistry
The Hebrew University of Jerusalem
Jerusalem 9190401, Israel
E-mail: netanel.shpigel@mail.huji.ac.il
F. Malchik
Center of Physical-Chemical Methods of Research and Analysis
al-Farabi Kazakh National University
Almaty 050012, Kazakhstan
E-mail: frodo-007@mail.ru
X. Wang
Storage of Electrochemical Energy (SEE)
Department of Radiation Science and Technology
Delft University of Technology
Delft 2629 JB, The Netherlands
E-mail: x.wang-22@tudelft.nl

that attracted considerable attention in the last years is $Ti_3C_2T_x$ (T_x stands for surface termination such as O, OH, and F) 2D compounds belonging to a large family of 2D transition metal carbides and nitrides named "MXenes". This new materials class contains a variety of MXene compositions like V_2CT_x,[3] Nb_2CT_x,[4] Mo_2C,[5] and Ti_2CT_x[6] which have recently shown unique characteristics and capabilities for energy storage and conversion. Yet, to date, the most studied MXene compounds remain to be $Ti_3C_2T_x$ owing to their superior electrochemical performance, expressed by high capacity, fast charging capabilities, and impressive long-term stability.[7] $Ti_3C_2T_x$ can be easily produced by selective etching of the Al layers from the raw Ti_3AlC_2 compound, typically by using HF-containing solutions (either directly in HF or in various fluoride salt combined with strong acids) to form Ti_3C_2 particles.[8] Usually, the obtained particles are delaminated into 2D flakes by mechanical treatment (e.g., shaking, sonication, rolling, etc.), or by chemical exfoliation methods in which large molecules (urea or dimethyl sulfoxide – DMSO for example) are inserted in between the MXene sheets.[9] This delaminated form of these materials provides not only improved electrochemical performance in terms of capacity and rate capability (as more surface area of the MXene particles becomes accessible for ions accommodation) but also opens better research opportunities for exploring intrinsic materials' properties even at a single flakes scale.[10] Many excellent review papers related to the preparation methods of MXenes,[11,12] characterizations of their unique physical and chemical properties,[13,14] and finally their use in energy storage applications,[15,16] have been recently published.

Yet, despite the inflation in the review papers about MXenes, we realized that there is no appropriate summary of the relevant findings related to the characterization of $Ti_3C_2T_x$ electrodes obtained by in situ techniques. As such analyses provide the most essential information regarding the charging mechanisms of $Ti_3C_2T_x$ electrodes and their associated structural and mechanical behavior, directly affecting their cycling performance, this review has two goals: presenting an overview of the in situ techniques used to characterize the electrochemical-induced changes that occur in $Ti_3C_2T_x$ electrodes and summarizing the main conclusions regarding the charging mechanisms of MXene electrodes in different electrolyte environments. Intelligent use of a combination of the relevant in situ techniques is in high demand to solve numerous problems related to the optimization of $Ti_3C_2T_x$ electrodes' cycling performance.

While various in situ methods were applied to study the processes occurring during the charge /discharge of batteries[17] and supercapacitors,[18] the electrochemical behavior of MXene electrodes possesses some unique properties related to their mechanical nature and morphological character, strongly influencing their charging mechanisms. As is further discussed, these properties clearly distinguish $Ti_3C_2T_x$ compounds from most electrode materials that are currently used in batteries and supercapacitors. Considering the significant influence of the electrolytic environments on the charge storage of the MXene electrodes, the first part of this review is devoted to the in situ characterization of $Ti_3C_2T_x$ electrodes in water-based electrolyte solutions including i) acidic ii) neutral iii) highly concentrated solutions and in iv) nonaqueous electrolyte as well. A

separate section focuses on v) the use of in situ tools to probe the mechanical properties of MXene electrodes induced by cations' insertion during charging processes. Finally, in section iv) we provide a discussion on the current challenges in the understanding of the charging mechanism of MXene electrodes in different operating environments and the use of various complementary analytical tools to expand and deepen our knowledge about their behavior.

2. Revealing the Charging Mechanisms of MXene Electrodes by In Situ Techniques

Unlike conventional batteries or supercapacitors electrodes that store charge via well-defined mechanisms, namely redox reactions, and electrostatic interactions respectively, the charge storage behavior of MXene electrodes originates from both faradaic and non-faradaic processes when in contact with electrolyte solutions.[19] Although the charge storage mechanisms of MXene electrodes are strongly dependent on their morphology and their surface chemistry,[20] it appears that the major factor dictating their electrochemical behavior is the electrolyte solution. In neutral electrolyte solutions, $Ti_3C_2T_x$ electrodes exhibit "capacitive-like" behavior expressed by rectangular cyclic voltammetry (CV) curves and linear capacitance changes with potential during galvanostatic polarization. For such electrolyte solutions, the total (integral) capacity values are determined by the electrochemical stability window of the electrolyte solution rather than by the storage capability of the MXene itself. In conventional electrolyte solutions (i.e., concentration of ≈1 M) the potential typically ranges between 0.2 to −0.8 V (vs Ag/AgCl) resulting in maximal capacity values ≈80–120 F g^{-1} (i.e., ≈18–20 mAh g^{-1}).[21] Further polarization induces hydrogen formation at the negative vertex and irreversible oxidation of the Ti atoms at the positive side. Recently it was demonstrated that utilization of highly concentrated electrolyte solutions, particularly saturated LiCl[22] and LiBr,[23,24] results in a significantly increased potential window of $Ti_3C_2T_x$ electrodes. This extended potential range is attributed to the suppressed hydrogen and oxygen evolution reactions in highly concentrated solutions,[25] resulting in improved capacities of the MXene electrodes up to 30 mAh g^{-1} (measured across the full potential window). In contrast, in acidic solutions, $Ti_3C_2T_x$ electrodes display a pseudocapacitive type of charging arising from redox reactions between the protons in the solutions and oxygen terminations of MXene electrodes which changes the Ti oxidation state. This reaction can be written in the following form:[26]

$$Ti_3C_2O_x(OH)_y F_z + \delta H^+ + \delta e^- \leftrightarrow Ti_3C_2O_{x-\delta}(OH)_{y+\delta} F_z \quad (1)$$
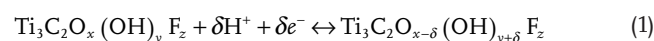
Such behavior results in significantly higher capacity values (≈350 F g^{-1}, equivalent to ≈90 mAh g^{-1} as demonstrated for MXene hydrogel electrodes[27]), reflected by well-expressed redox peaks in the voltammograms of these systems and pronounced dependence of the slopes of the galvanostatic charge-discharge (GCD) curves on the applied voltage. Finally, in aprotic electrolytes where lower negative potentials can be approached, the response is mainly attributed to redox interactions between the
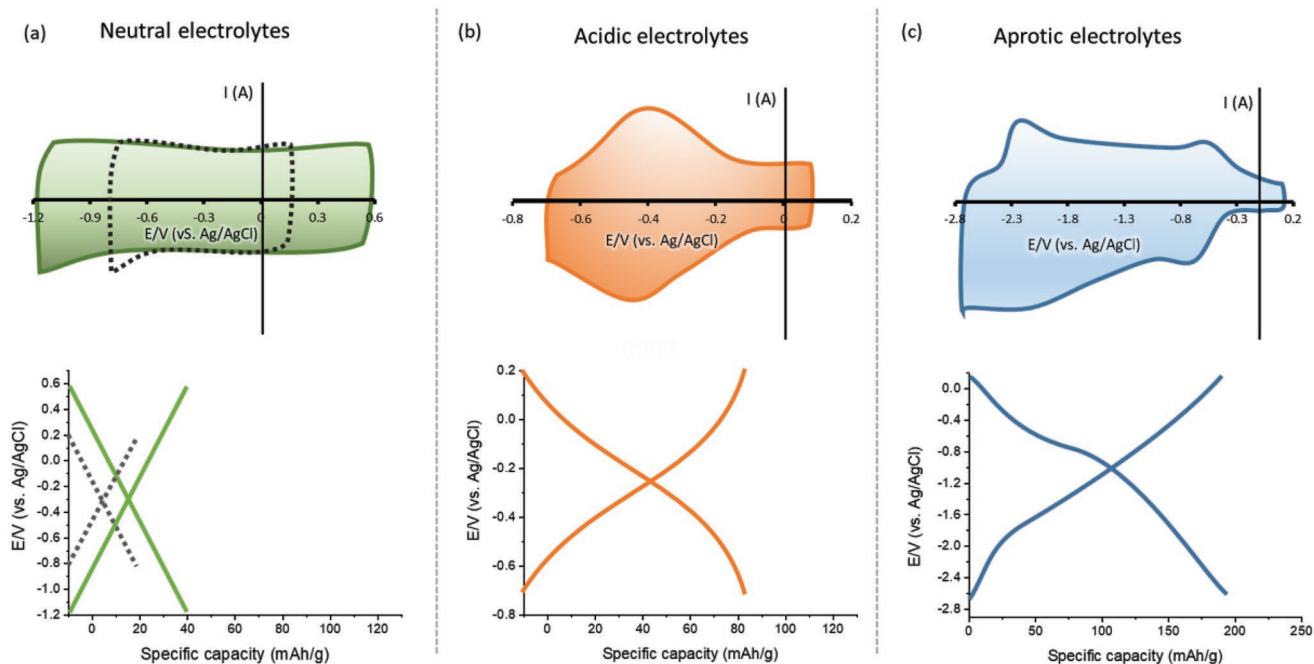
Figure 1. Typical schematic CV and GCD plots of $Ti_3C_2T_x$ electrodes in a) neutral aqueous standard 1 M (dashed lines) and concentrated electrolytes b) acidic aqueous electrolytes and c) non-aqueous electrolyte solutions.
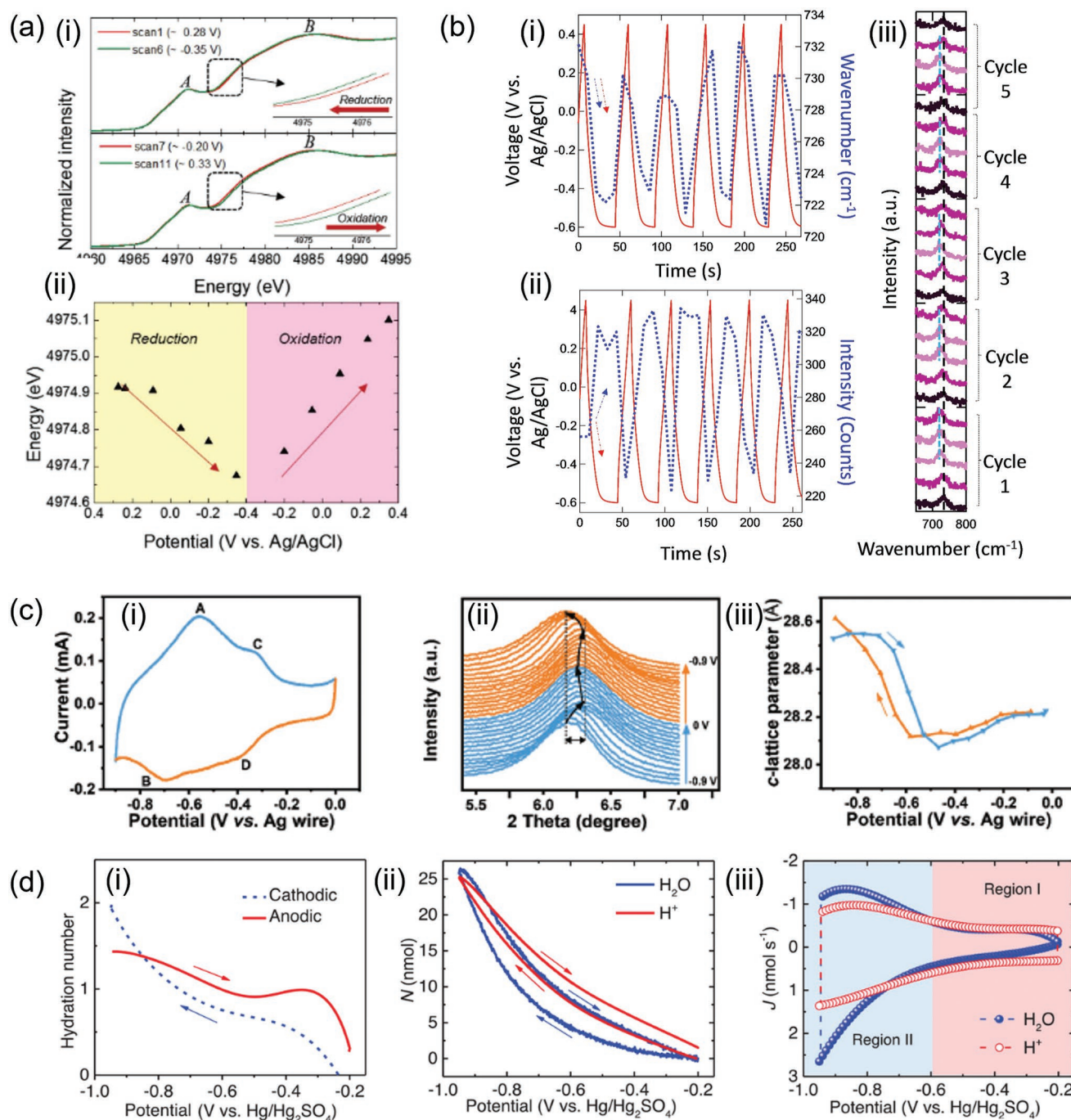
intercalated ions to the MXene's surface termination groups which practically induces variations in the Ti oxidation state.[28] The pseudocapacitive character of the MXene electrodes in non-aqueous electrolyte solutions is reflected by distorted capacitive cyclic voltammetric curves and the nonlinear GCD profiles. It is worth noting that due to the large versatility of non-aqueous electrolyte systems, and the strong influence of the MXenes' properties on the interfacial solid-liquid interactions, one cannot define a typical CV/GCD response for these systems. Considering this comment, **Figure 1**a,b depicts schematic CV and GCD profiles of $Ti_3C_2T_x$ electrodes in aqueous neutral and acidic electrolyte solutions. A possible response of MXene electrodes in aprotic solutions (adapted according to ref. [29]) is presented in Figure 1c.

Given the above, the following sections describe the main findings acquired by various in situ techniques related to the electrochemical behavior of MXene electrodes in acidic, neutral, and aprotic solutions.

3. MXene Electrodes in Acidic Electrolyte Solutions

Several in situ techniques including X-ray absorption near edge structure spectroscopy (XANES), XRD, in situ Raman, and electrochemical quartz crystal microbalance with dissipation monitoring (EQCM-D) were applied to reveal the charging mechanisms of MXenes in acidic aqueous electrolyte solutions. In situ XANES measurements conducted in 1 M H_2SO_4 solutions showed a shifting of the Ti edge spectra toward lower energies upon negative polarization and positive shifting back to the original energy at the reverse scan.[30] This indicates reversible changes in the Ti oxidation state under acidic conditions

as presented in **Figure 2**a. Based on these observations, an average change of $0.1\overline{e}$ per Ti for a 0.7 V voltage window was estimated, corresponding to a capacitance value of 205 F g^{-1}. A similar trend was also recognized in recent in situ XANES studies conducted by Shao et al. which showed slightly larger changes of $0.134\overline{e}$ in the Ti oxidation state when a larger potential window was applied (0.9 V).[31] These findings are in line with in situ Raman studies conducted for acidic electrolyte solutions (0.1 M HCl)[32,33] As can be seen in Figure 2b significant voltage-dependent changes of the Raman spectra, expressed by a continuous red shifting of the 730 cm^{-1} bands toward a lower wavenumber of 722 cm^{-1} were detected upon scanning of the potential from 0.4 to −0.6 V (vs Ag/AgCl). These variations in the observed spectra are attributed to the transition of $Ti_3C_2O_2$ to $Ti_3C_2O(OH)$. As the 722 cm^{-1} peaks were located between the −O− and the −OH vibration modes (positioned at 732 cm^{-1} and 715 cm^{-1} respectively), it was concluded that only partial protonation of the −O− termination takes place in this electrolyte solution. During reverse anodic charging, the peaks were shifted back to their original position associated with the deprotonation of the $Ti_3C_2T_x$. Interestingly, in the limited cathodic range (down to −0.45 V) significant changes in the Raman spectra were detected. Based on this observation one can assume the occurrence of two charging mechanisms – double layer adsorption of protons which takes place at a positive potential range, and the subsequent protons-induced surface redox reaction at more negative potentials.[32] The morphological changes of MXene films during proton insertion/extraction were further evaluated by in situ XRD measurements.[34] It was found that the changes of the interlayer spacing of the $Ti_3C_2T_x$ films are strongly affected by the applied voltage – upon charging to −0.6 V a lattice shrinking of 0.1 Å was probed, while further polarization to more negative potentials resulted

**ADVANCED
SCIENCE NEWS**

www.advancedsciencenews.com

**ADVANCED
ENERGY
MATERIALS**

www.advenergymat.de

Figure 2. In situ characterization of MXene electrodes in an acidic environment. a) i) Ti K-edge XANES spectra recorded during positive and negative polarization of $Ti_3C_2T_x$ electrode in 1 M H_2SO_4 ii), variation of Ti edge energy as a function of the applied potential. Reproduced with permission.[30] Copyright 2015, Wiley b) The changes in the wavenumber i) and the peaks intensity ii) recorded by in situ Raman spectra upon cycling of $Ti_3C_2T_x$ electrodes in 0.1 M HCl, iii) the variation in the recorded spectra during 5 cycles. Reproduced with permission.[32] Copyright 2022, Wiley c) in situ XRD analysis of MXene electrodes in 1 M H_2SO_4: i)CV response, ii) XRD patterns collected during charging/discharging, iii) the corresponding variation in the d spacing with the applied potential. Reproduced with permission.[26] Copyright 2019, Wiley d) in situ EQCM measurements of MXene electrodes in 1 M H_2SO_4 solution: i) calculated hydration number of the inserted protons and the total ions population ii) as a function of potential, iii) H^+ related ionic flux (red) and total ionic flux (blue) versus potential. Reproduced with permission.[35] Copyright 2022, Wiley.

in a significant expansion of the interlayer space by 0.1 Å (see Figure 2c). Using DFT simulations this fluctuating response was ascribed to the presence of two types of surface terminations, namely −O, and −OH: the former tends to shrink upon

H^+ insertion while OH− terminated $Ti_3C_2T_x$ expands. These observations are consistent with recent in situ EQCM studies conducted by Lin et al.[35] As demonstrated, the characterization of $Ti_3C_2T_x$ films in acidic environments (1 M H_2SO_4) reveals a
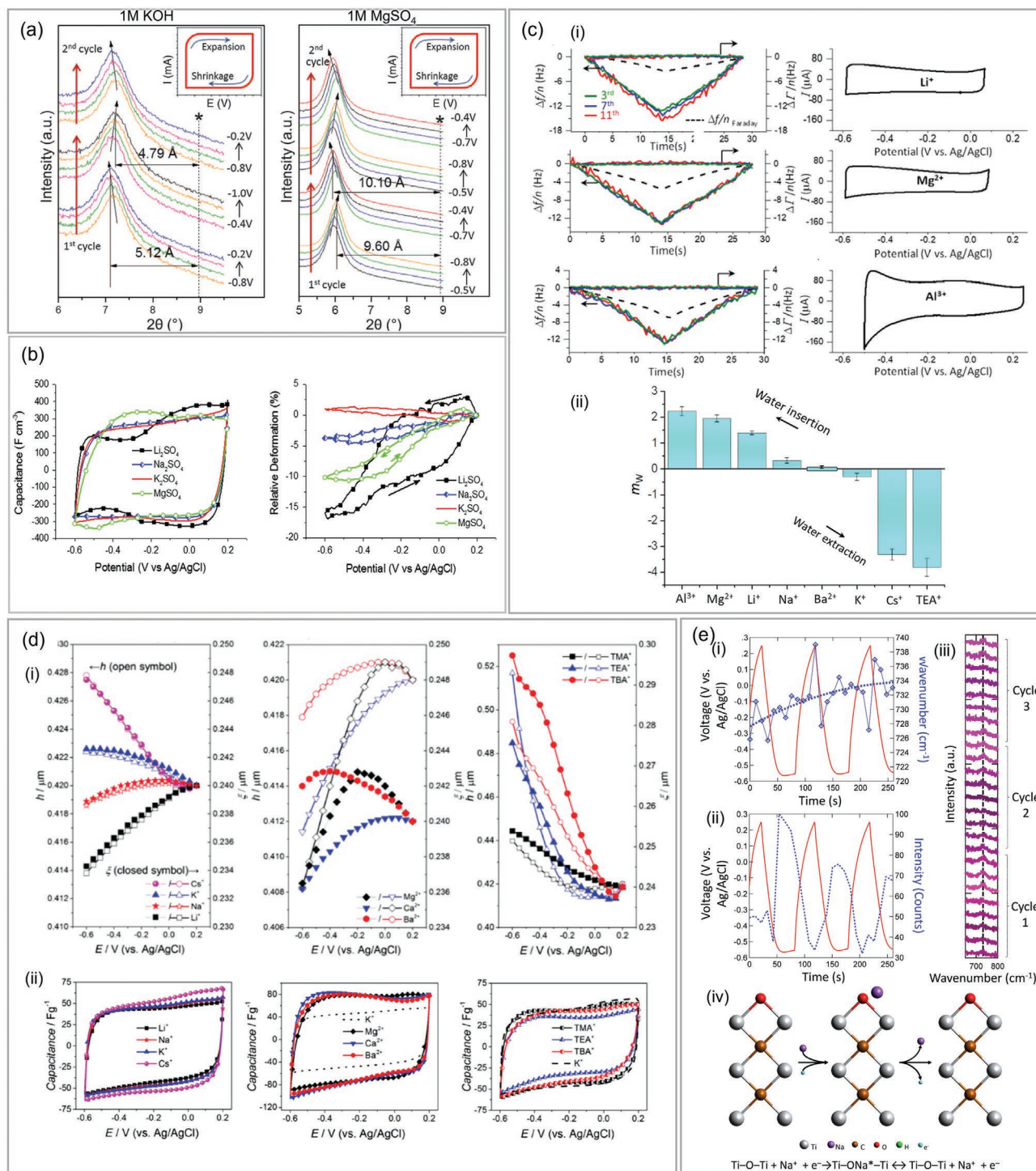
potentially dependent gravimetric response attributed to the varied hydration state of the inserted protons. As can be seen in Figure 2d polarization from −0.2 to −0.6 V resulted in co-insertion of 0.72 H_2O per H^+ in (region I) while an increased H_2O/proton ratio of 1.45 was measured in region II. Considering the above-mentioned XRD measurements which show expansion of the layer below −0.6 V, one can attribute the increased H_2O amount to the enlarged interlayer spacing of the MXene particles in such negative potentials.[35] In fact, the influence of the confined water on the charging mechanism of MXene in an acidic environment seems to be significant. Based on DFT calculations it was found that the presence of water in between the MXene layers facilitates its charging kinetics by providing a hydrogen-bonded water network for fast proton diffusion, probably via a Grotthuss-type mechanism.[31]

4. MXene Electrodes in Neutral Aqueous Electrolyte Solutions

In contrast to acidic solutions in which the capacity of the MXene electrodes is attributed to faradaic interactions between the protons and the surface terminating groups, the charge storage mechanism in neutral solutions is still under debate. The main difficulty in this regard is the origin of the high capacitance (100–150 F g^{-1}) of the MXene electrodes in neutral electrolyte solutions, despite their relatively small surface area. While a similar capacitance range is typically observed for highly porous activated carbons in neutral aqueous solutions,[36] these compounds are characterized by extremely high surface area (typically more than 2000 m^2 g^{-1}).[37] Such large surfaces provide an enormous amount of adsorption sites for electrolyte ions, leading to a high specific capacitance of electrodes comprising activated carbons. In contrast, typical MXene electrodes have a significantly lower surface area, usually, a few to tens m^2 g^{-1}, [38,39] questioning their charging mechanism.

Unlike many conventional metal oxide intercalation compounds defined by rigid crystalline structures with limited volume change tolerance for large ions insertion, MXenes structure can accommodate large structural deformations without severe mechanical degradation. This property of MXenes raised more questions about the influence of ions type and their solvation character on the charging performance and the associated physical phenomena of the $Ti_3C_2T_x$ electrodes. Upon cation insertion either by potential application or by spontaneous ions exchange,[40] the interlayer distance between the adjacent layers is varied according to the size and the valence of the intercalated ions. Preliminary in situ XRD measurements[41] taken during intercalations of K^+ and Mg^{2+} in 1 M KOH and $MgSO_4$ aqueous solutions showed intermittent reversible expansion/contraction of MXene electrodes during their positive and negative polarization (see **Figure 3**a). This behavior was attributed to the incorporation of cations between the negatively charged MXene sheets, which result in increased attraction between the $Ti_3C_2T_x$ layers. These findings are in good agreement with further in situ atomic force microscopy (AFM) measurements conducted in various sulfate-based electrolyte solutions containing Li^+, Na^+, K^+, and Mg^{2+}.[42] The observed deformation patterns indicated a contraction of the MXene electrodes upon insertion of Li^+ Mg^{2+} and Na^+ ions and expansion during the reverse process when positive potentials were applied. As can be seen in Figure 3b the largest variation in the electrodes' dimensions was detected for intercalation of Li^+ ions, while smaller changes were observed upon insertion of Mg^{2+} and Na^+ ions. Having the highest hydration radius among the investigated ions (≈4.28, 3.58, and 3.82 Å, for Mg^{2+}, Na^+, and Li^+, respectively),[34] it was anticipated that Mg^{2+} ions intercalation would result in a greater expansion. Note, however, that the hydration radius of the ions in the bulk electrolyte solutions may differ substantially from their hydration radius in the confined space. It is, therefore, reasonable to assume that Mg^{2+} ions are partially stripped of their solvation shell upon insertion into the MXene structure, resulting in a smaller effective radius than that of Li ions. Interestingly, in contrast to previously described ions, only a slight expansion of MXene electrodes was detected during the intercalation of K^+ ions. This behavior was also supported by ex situ XRD measurements which demonstrated significant changes in the d-spacing of $Ti_3C_2T_x$ upon Li^+ ions insertion, while only minor variations in the case of K^+ ions insertion.[33] These results were further confirmed by in situ electrochemical dilatometry which shows significant volume contraction (up to 23%) during Mg^{2+} ions insertion while only small volume deformation for K^+ ions insertion.[43] As the hydrated radius of K^+ is the smallest among the examined ions (i.e. 3.31 Å) the last finding cannot be ascribed to this parameter. Indeed, in situ EQCM-D measurements performed by Shpigel et al, revealed complex dynamics upon ions insertion into MXenes.[44] Based on the differences between the experimental and the predicted frequency changes (the latter value can be easily determined by combining Sauerbrey and Faraday equations) it was found that the ions insertion is strongly influenced by the kosmo/chaotropic character of the inserted ions. As kosmotropic ions are characterized by large charge density (i.e., high charge-to-size ratio) they have strong solvation interactions. Hence, these ions are inserted into MXenes in partially solvated form resulting in a larger experimental frequency change than the predicted one (dashed lines in Figure 3c-i). According to their solvation energies, the amount of the co-inserted water has been found to change in the following order Al^{3+} > Mg^{2+} > Li^+ ions insertion. It is worth mentioning that the hydration number of these ions in the electrolyte solutions' bulk is significantly different from the hydration number of the inserted cations, indicating their partial desolvation upon intercalation into MXenes. In contrast, the insertion of chaotropic (i.e., weakly solvated) cations characterized by large ionic radii resulted in the expulsion of water molecules out of the MXene layers, where the largest number of expelled water was calculated for Cs^+ and TEA^+ which have the largest ionic radius among the studied cations, as summarized in Figure 3c-ii These findings were later confirmed by ab initio molecular dynamics calculations (AIMD) performed by Gao et al., who demonstrated that when the distance between neighboring oxygen atoms in the cations' solvation shell is larger than the cation-water bond length, co-insertion of water molecules is expected. Oppositely, when the cation-water distance is larger (as in the case of K^+ and Cs^+) water should be expelled from the MXene nano slits.[45] These observations suggest that the insertion of cations into MXenes does not depend on a sole parameter such as hydration radius, or ion's charge.

ADVANCED
SCIENCE NEWS

www.advancedsciencenews.com

ADVANCED
ENERGY
MATERIALS

www.advenergymat.de

Figure 3. In situ characterization of MXene electrodes in aqueous neutral electrolyte solutions: a) in situ XRD spectra collected for Ti_3C_2 electrodes cycled in aqueous 1 M KOH and $MgSO_4$ solutions. Reproduced with permission.[4] Copyright 2013, AAAS b) CVs and relative electrode deformations recorded during in-situ AFM measurements in various aqueous electrolytes. Reproduced with permission.[42] Copyright 2015, Elsevier c) i) in situ EQCM-D results showing the variations in frequency and dissipation upon insertion/extraction of Li^+, Mg^{2+}, and Al^{3+} ions into MXene films (the theoretical frequency changes are represented by the dashed black line). The corresponding CVs are shown alongside ii) the calculated ratio of inserted cations to co-inserted water molecules (designated as M_w) for various investigated ions; Reproduced with permission.[48] Copyright 2018, American Chemical Society d) in situ morphological characterizations of MXene particles obtained by EQCM. The related variations in the effective electrode thickness $-h$ and permeability length $-\xi$ and the obtained CVs for various monovalent and divalent ions are presented in panels (i) and (ii); Reproduced with permission.[49] Copyright 2014, Wiley e) The changes in the wavenumber (i) and the peaks intensity ii) recorded by in-situ Raman spectra upon cycling of $Ti_3C_2T_x$ electrodes in 0.5 M Na_2SO_4, iii) the variation in the recorded spectra during 5 cycles and iv) atomistic description of the proposed charging mechanism. Reproduced with permission.[32] Copyright 2022, Wiley.

**ADVANCED
SCIENCE NEWS**

www.advancedsciencenews.com

**ADVANCED
ENERGY
MATERIALS**

www.advenergymat.de

Instead, a more complicated description that takes into account the behavior of the hydrated ions and the water molecules in the confined space should be carefully considered.

Additional information about how different cations affect the structural deformations of MXene electrodes was provided by in situ EQCM measurements conducted for composite electrodes consisting of multilayered (essentially not delaminated) $Ti_3C_2T_x$ particles.[46] Unlike the previous EQCM-D study which focused on the gravimetric changes (i.e., the only variation in mass) this research concentrated on the morphological changes induced by the polarization of MXene electrodes. This operation mode of EQCM-D takes into account the hydrodynamic interactions between the acoustically-induced oscillation of the electrodes' coating (thin layers comprising MXene particles) and the contacting electrolyte solution.[47] These solid-liquid interactions varied with the changes in the morphology of the electrodes giving a rise to changes in the resonance frequency width. By application of suitable hydrodynamic modeling, one can correlate the changes in the frequency and the frequency width with the morphological variations of the electrodes. Using this approach, the changes in the effective thickness $-h$ and the effective porosity $-\xi$ of the MXene structure were monitored for a large variety of alkaline, alkaline earth, and tetraalkylammonium cations. As displayed in figure 3d-i capacitive-type response CVs were observed for all the examined systems. The main conclusions from changing the parameters h and ξ for the examined cations presented in figure 3d-ii are as follows: for the cations with a high charge-to-size ratio, both thickness, and porosity decrease during negative polarization owing to enhancement of the electrostatic attraction between the MXene sheets. An opposite trend (expansion of the electrode during ion insertion) can be clearly seen for the cations with a small charge-to-size ratio. A mixed tendency was observed for the insertion of double-charged cations: at the beginning of the cation's insertion (when their population in the MXene interspace is small) their large size plays the dominant role whereas as their population increases, the double-charge of the cations enhances attraction between the neighboring MXene sheets.

Attempting to understand the charging mechanism in neutral electrolyte solutions, recent in situ Raman studies were conducted for delaminated $Ti_3C_2T_x$ electrodes in 0.5 M Na_2SO_4.[33] As can be seen in Figure 3f no changes in the vibration bands associated with the $-O-$ terminations (positioned at the 730 cm^{-1} region), indicating a double layer type charge storage mechanism.

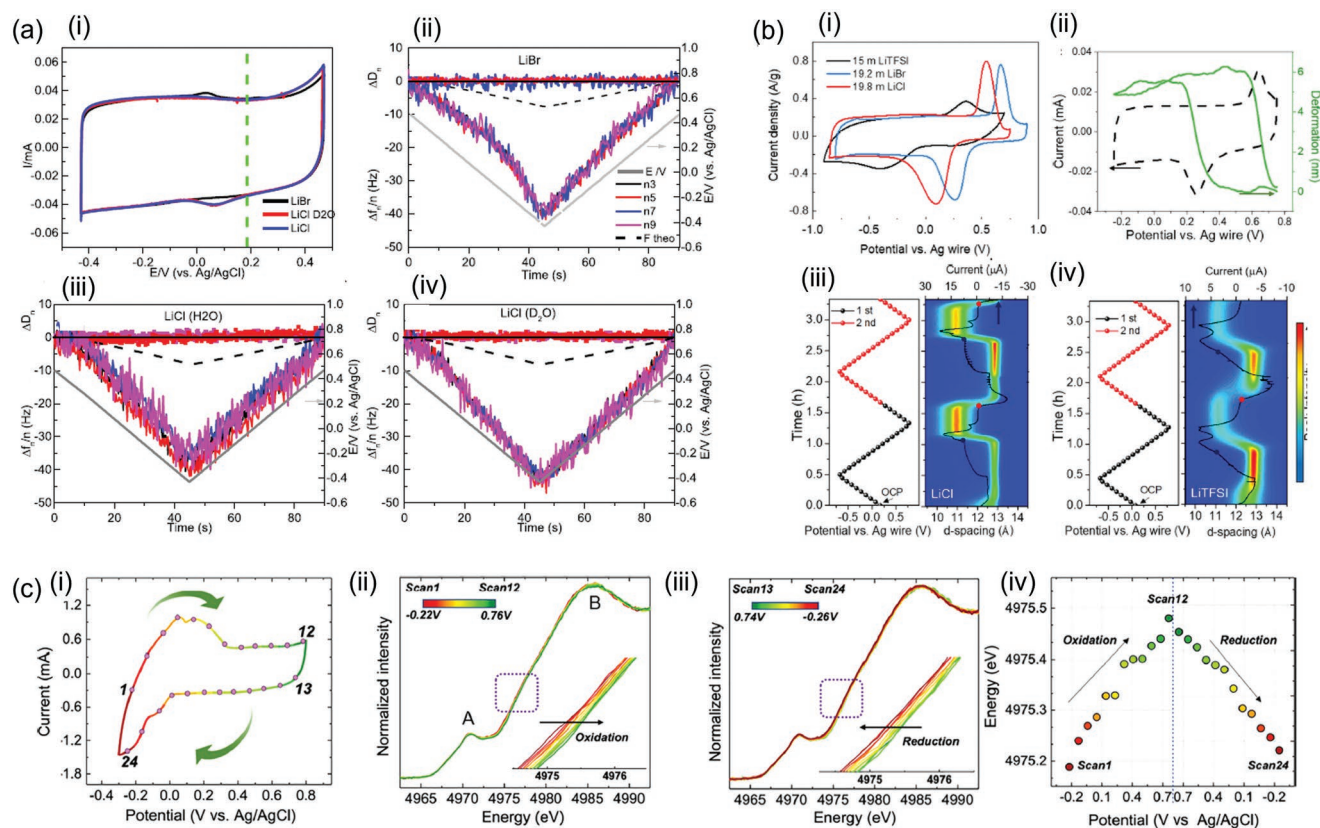## 5. MXene Electrodes in Highly Concentrated Aqueous Electrolyte Solutions

The recent discovery of the "water-in-salt" (WIS) concept,[25] which utilizes highly concentrated electrolyte solutions to get an extended electrochemical stability window, opened new research directions for the characterization of MXene electrodes in neutral electrolyte solutions. As demonstrated by Malchik et al.,[21] the use of 14 M LiCl solutions resulted not only in the increased overpotential of H_2 generation on the cathodic side but also improved the oxidation stability of the MXene electrodes on the positive side. This enlarged potential

window (ranges between −1 to 0.6 V vs Ag/AgCl) resulted in high-capacity values of the $Ti_3C_2T_x$ and lead to the discovery of new phenomena related to the operation of MXene electrodes in such concentrated solutions.

The extended positive window in these systems for the $Ti_3C_2T_x$ electrodes allows addressing a key issue related to the possibility of anions insertion into the MXene electrodes. Based on in situ EQCM-D measurements of MXene films in saturated LiBr and LiCl solutions, it was concluded that anions cannot be inserted into MXene electrodes. As seen in **Figure 4**a, scanning from a positive to the negative vertex in saturated LiCl, resulted in a negative frequency shift, that only cations were inserted into the MXene electrodes. In the opposite scanning direction, a continuously increasing frequency shift was detected attributed to the extraction of cations. A similar frequency trend was measured for LiBr solutions implying that anions cannot be inserted into the MXene structure. This finding was further confirmed by in situ XRD measurements which showed a gradual contraction of the MXene electrodes upon charging from the negative to the positive vertex.[23] Based on DFT calculations it was shown that the insertion of anions into MXene electrodes is not energetically favorable due to the presence of negatively charged termination groups on the MXenes surface. Similar to the above-mentioned gravimetric EQCM-D study, the number of the co-inserted water molecules was calculated by comparing the theoretical frequency (dashed lines in Figure 4a) and the experimentally measured values. Interestingly, a ratio of 1.4 water molecules per single Li ions was found for saturated LiCl similar to the ratio that was found for Li ions insertion in the diluted solutions.[50] Considering the higher solvation degree in diluted electrolytes, this finding suggests that only part of the first solvation shell is co-inserted into the confined space of MXene.

The number of the co-inserted water molecules changes with applied potential in the $Ti_3C_2T_x$ – WIS systems.[50] A "redox-like" charge storage process was observed with MXene electrodes, as indicated by a pair of pronounced and separated peaks in the related CV curves (Figure 4b). Using in situ XRD complemented by in situ AFM, the redox-like process was found to be correlated with the Li^+ intercalation and deintercalation though the process occurs at a potential positive than the open circuit potential. Further, in situ EQCM-D measurements estimated the amount of the co-inserted water molecules to be ≈2.8 H_2O: Li^+ which is much higher than the ratio at other potentials (≈1.4). A large amount of the co-inserted water at this positive potential range is well correlated with the dramatic interlayer distance change observed by XRD (see Figure 4b-iii). As well correlated with the AFM findings (see Figure 4b-ii) insertion/ extraction of Li^+ ions from concentrated electrolyte solutions results in expansion/contraction of MXene layers. Interestingly, an opposite trend was measured in diluted solutions (contraction upon Li^+ ions insertion and vice versa, see Figure 3b). Such a difference may be attributed to the stronger coordination of the water to the cations in the WIS environment which prevents the distribution of the inserted water inside the MXene layers. Surprisingly, despite the pronounced redox-like CV response, the behavior of MXene electrodes in saturated electrolyte solutions cannot be ascribed to the Faradaic process. As further approved by in situ ultraviolet-visible spectroscopy, only

**ADVANCED
SCIENCE NEWS**

www.advancedsciencenews.com
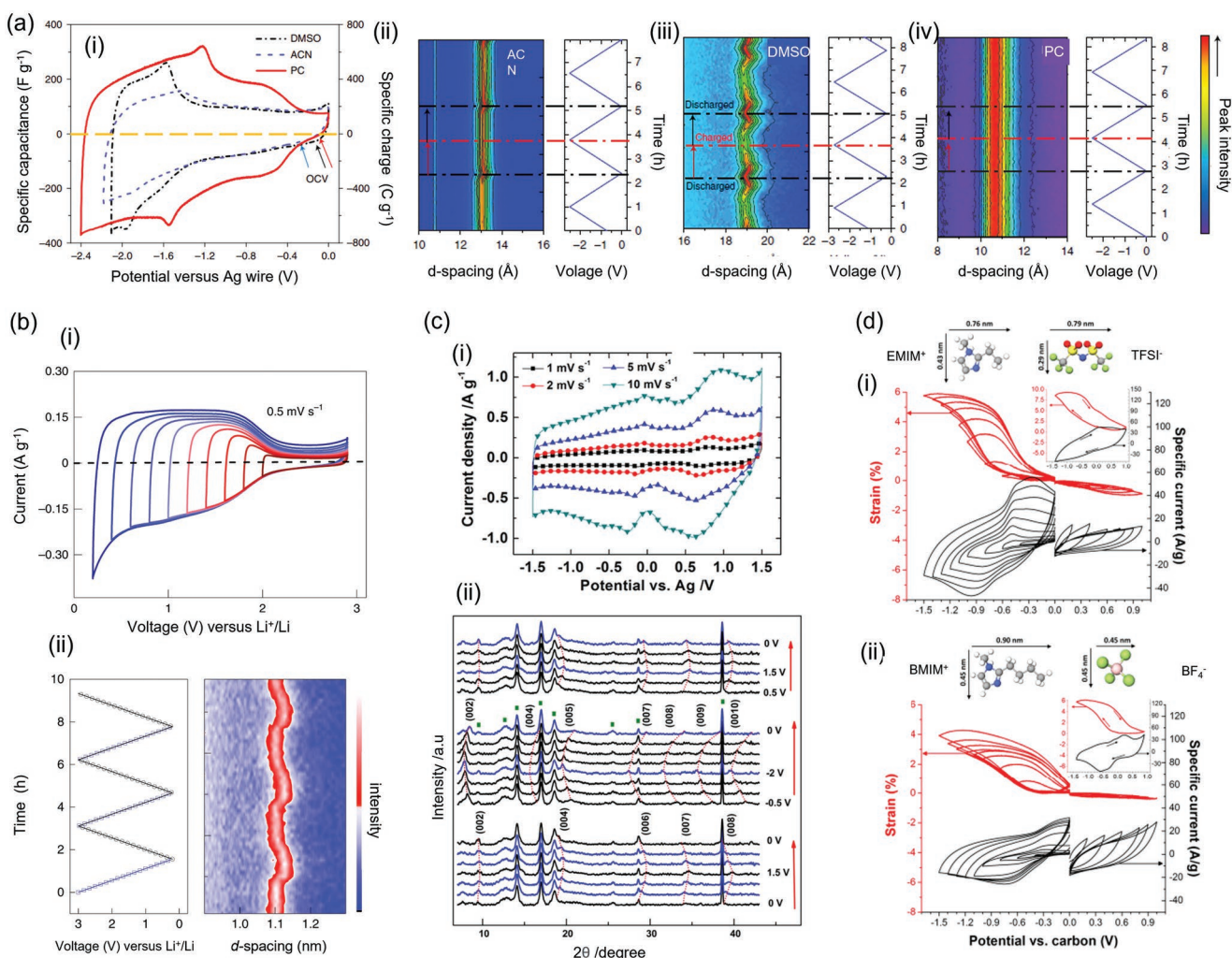
**ADVANCED
ENERGY
MATERIALS**

www.advenergymat.de

Figure 4. In situ characterization of MXene electrodes in highly concentrated aqueous solutions: a) i) CVs of MXene-coated quartz sensors and the corresponding frequency and dissipation changes (measured by EQCM-D) in concentrated ii) LiBr iii) LiCl in H_2O and iv) LiCl in D_2O; Reproduced with permission.[23] Copyright 2021, American Chemical Society b) Behavior of $Ti_3C_2T_x$ electrodes in highly concentrated LiCl, LiBr, and LiTFSI (i), cyclic voltammograms (ii) Deformation of MXene electrodes in sat. LiCl measured by in situ AFM. In situ XRD spectra were collected upon cycling MXene electrodes in highly concentrated (iii) LiCl, and (iv) LiTFSI. Reproduced with permission.[50] Copyright 2021, American Chemical Society c) CV (i) and in situ XANES spectra obtained during oxidation (ii) and reduction of (iii) $Ti_3C_2T_x$ in concentrated (19.2 m) LiBr. The calculated changes in the Ti K-edge energy as a function of the applied potentials are shown in (iv). Reproduced with permission.[52] Copyright 2021, American Chemical Society.

minor changes in the Ti oxidation state were observed in WIS electrolytes. On the contrary, much stronger shifts in plasmon resonance peaks were observed in both acidic electrolytes, indicating strong surface redox reactions in this environment.[51]

Surface redox can be introduced into the MXene-WIS electrolyte systems when the MXenes are slightly oxidized.[52] By electrochemical oxidation $Ti_3C_2T_x$ electrodes at ≈1.3 V versus Ag in the WIS systems, a pair of peaks emerge in the CV curves at negative potentials (Figure 4c). These peaks correspond to a reversible surface redox reaction, as confirmed by the in situ Ti K-edge XANES. Over a potential window of 1.1 V, the average Ti oxidation state changes by 0.08 $\bar{e}$ per Ti atom, which contributes to a capacitance of 104 F g^{-1}. The surface redox activated in the neutral aqueous electrolyte is due to the increased Ti valence of the slightly oxidized MXene. Besides, in situ extended X-ray absorption, fine structure measurements (EXAFS) can further reflect the charge storage mechanism implying local structural changes in the MXenes. The interatomic distance of Ti-C and Ti-Ti shrink and expand reversibly during the charge/discharge process based on the EXAFS measurements. The distance changes are associated again with Ti valence state changes, which offers evidence of the presence of surface redox reactions.

6. MXene in Nonaqueous Electrolyte Solutions

In situ measurements of MXene electrodes in contact with non-aqueous electrolyte solutions provide valuable information about the effect of the ion's solvation on the charging mechanism and the associated changes in its interlayer spacing. The influence of the solvents' nature on the volume variations of $Ti_3C_2T_x$ electrodes was recently assessed by Wang et al.[29] In this study, 1 M LiTFSI salt was dissolved in 3 different solvents, namely propylene carbonate (PC), acetonitrile (ACN), and dimethyl sulfoxide (DMSO). As can be seen in **Figure 5**a-i, significant differences in the measured capacities were observed where the highest capacitance was observed for PC-based electrolyte solutions, that is, 195 F g^{-1} versus 130 F g^{-1}, and 110F g^{-1} for DMSO and ACN, respectively. As found by in situ XRD measurements, the application of negative polarization from the open-circuit voltage (OCV) to -1 V (vs Ag wire) results in expansion of the electrode's d-spacing for ACN and DMSO (Figure 5a-ii,iii respectively) and shrinking during positive polarization. In contrast, no volume changes were detected upon polarization in PC-based systems (Figure 5a-iv). Based on these findings, the differences in the MXenes structure were ascribed to the presence of co-inserted solvent molecules

ADVANCED
SCIENCE NEWS

www.advancedsciencenews.com

ADVANCED
ENERGY
MATERIALS

www.advenergymat.de

Figure 5. In situ characterization of MXene electrodes in non-aqueous electrolyte solutions: a) Cyclic voltammograms (i) and the corresponding d-spacing variations measured by in situ XRD of MXene electrodes in ACN, DMSO, and PC solutions containing 1 M LiPF$_6$ (ii, iii, iv respectively); Reproduced with permission.[29] Copyright 2019, Nature Publishing Group (b) i) CV response and in situ XRD spectra ii) of Ti$_3$C$_2$T$_x$ particles prepared via molten salt synthesis; Reproduced with permission.[54] Copyright 2021, Nature Publishing Group c) in situ XRD spectra (i) and the cyclic voltammograms (ii) collected for Ti$_3$C$_2$ electrodes during cycling in EMIM-TFSI; Reproduced with permission.[55] Copyright 2016, Elsevier d) displacement changes of MXene electrodes measured by in situ dilatometry during positive and negative potential scans in i) EMIM-TFSI and ii) BMIM-BF$_4$ ionic liquids. Reproduced with permission.[56] Copyright 2016, American Chemical Society.

between the MXene sheets which were found to be to a larger extent in DMSO solutions. In contrast, in PC-based solutions, it seems that Li$^+$ ions are forced to strip their solvation shell and hence more space in the MXenes' structure remains available for cations insertion resulting in higher specific capacity values. The surface chemistry of Ti$_3$C$_2$T$_x$ has a strong influence on their electrochemical behavior and the interlayer space change when cycling in the Li-based organic electrolyte solutions. The successful development of the molten salt synthesis route of MXenes enables the fabrication of halogen-terminated MXenes. Unlike conventional MXene electrodes synthesized via solution etching process hydrofluoric acid, the MXenes etched by the molten salt with Lewis acid properties results in the formation of surface functional groups associated with the anion of the Lewis acid and oxygens.[53] As depicted in Figure 5b-i, The CV curves of the Cl$^-$ terminated Ti$_3$C$_2$ in 1M LiPF$_6$ in

1:1 v/v EC: DMC electrolyte solution shows a rectangular shape from the OCV to 2 V (vs Li$^+$/Li), which expanding dramatically toward lower potentials. The high-capacity value of 205 mAh g^{-1} of the molten salt synthesized MXene has been ascribed to the absence of OH$^-$ groups on the Ti$_3$C$_2$T$_x$ surface and the favorite formation O- terminations in this synthesis route. It was assumed that the presence of the latter species leads to effective interactions between O and Li resulting in improved electrodes' capacity.[54] In situ XRD reveals that the d-spacing of MXenes is roughly constant at ≈11 Å with a maximum change of 0.25 Å during cycling (as shown in Figure 5b-ii). The small d-spacing of MXenes indicates the intercalation of desolvated Li$^+$ between the MXene layers, which leads to compact interfacial Li$^+$ storage and high capacity.

The behavior of MXene electrodes in ionic liquids was monitored by Lin et al. in 1-ethyl-3-methylimidazolium

bis-(trifluoromethylsulfonyl)-imide (EMITFSI)[55] and by Jackel et al.[56] in EMIM-TFSI and BMIM-BF$_4$ ionic liquids. Based on the obtained XRD results, it seems that MXenes undergo expansion during cation insertion and contraction upon their extraction for all the examined systems (see Figure 5c-ii). This was well expressed by a negative shifting of the 002 peaks when negative potentials were approached and the opposite shift during the reverse positive voltage scan. Interestingly, a further reduction in the interlayer spacing was observed when electrode potential was scanned positively (relative to the initial OCV value). Such a behavior can be explained by the additional extraction of cations from the MXenes' structure. Further in situ dilatometry measurements applied to MXenes in contact with both EMIM-TFSI and BMIM-BF$_4$[56] demonstrate a gradual increase in the measured strain during negative potential scans, while the opposite trend was observed during the course of the reverse scans, consistent with the XRD results. As shown in Figure 5d-i,ii, the application of positive potentials with respect to the OCV leads to a further reduction of the electrode strain in both BF$_4^-$ and TFSI$^-$ based ionic liquids suggesting that only cations are extracted at positive potentials[56] as demonstrated for aqueous electrolyte solutions.

7. In Situ Potential-Dependent Viscoelastic Changes in Ti$_3$C$_2$T$_x$ Electrodes

The unique mechanical character of Ti$_3$C$_2$T$_x$ electrodes, particularly its high elasticity (a theoretical Young's modulus of 502 GPa was predicted by molecular dynamics simulations, while more than 300 GPa was measured by AFM indentation[57]) and its high tensile strength[58] (a value of 570 MPa was measured for 940 nm thick MXene film), triggered research into the electrochemical-mechanical coupling of MXene electrodes. Apart from the scientific importance of such research, this study should also have practical applications for the development of MXene-based electrochemical actuators.[59]

The main tool for in situ morphological characterizations of MXene electrodes is AFM.[60] Come et al. employed contact resonance (CR) frequency AFM imaging[61] to quantify the elastic properties of Ti$_3$C$_2$T$_x$ (MXene) paper electrodes during electrochemical cycling.[42] **Figure 6**a represents the CR-AFM experimental setup used for tracking the resonance frequency as a function of the position and state of charge of the electrode using the band excitation technique to quickly measure contact resonance cantilever dynamics while scanning. The cantilever response to the multifrequency photothermal excitation was detected and Fourier transformed to identify the CR frequency at every point of the scan. The interest in studying the mechanical changes of Ti$_3$C$_2$T$_x$ comes from its lattice variations while cation intercalation occurs in aqueous solutions together with the co-insertion of water molecules. In situ CR-AFM measurements of MXene films in aqueous Li$_2$SO$_4$ and K$_2$SO$_4$ electrolyte solutions revealed distinct variations in their elastic modules during charging/discharging.[62] While a continuous increase in the elastic modulus upon scanning to the negative potentials (up to −0.8 V vs Ag/AgCl) was recorded in both solutions, higher stiffening (larger elastic modules) was measured in Li$_2$SO$_4$ as compared to K$_2$SO$_4$. This is due to the larger MXene

contraction during Li$^+$ insertion, as opposed to K$^+$ intercalation, which only results in minor volume changes (see figure 3). Intestinally, as seen in Figure 6b, inhomogeneous variations in the elastic properties were identified for the intercalated electrodes. Such behavior was ascribed to the presence of shallow and deep intercalation sites resulting in non-uniform cations intercalation, as was found earlier by in situ EQCM measurements.[46] As the shallow sites provide facile ions transport pathways, these intercalation sites experience higher stiffing than the deep ones in the less accessible regions. Based on the obtained stiffening mapping, the elasticity variations at the deep and the shallow insertion sites were analyzed as shown in the bottom panels in Figure 6b.

A subsequent in situ AFM study, conducted by Gao et al.[43] reveals that pre-insertion of K$^+$ ions into MXene electrodes leads to more uniform deformations and mechanical variations upon Mg^{2+} ions intercalation. Interestingly, the K$^+$ pre-intercalated MXene showed not only improved mechanical properties but also improve capacity and rate capability values as can be seen in Figure 6c.

Another effective in situ tool enabling monitoring of the mechanical properties of operating electrodes is EQCM-D. We have already described the use of EQCM-D as a gravimetric probe for the electrochemical insertion of a large variety of kosmotropic and chaotropic cations into thin MXene electrodes (Figure 3c). Later we discussed the use of this technique for highly sensitive hydrodynamic probing of intercalation-induced dimensional and porous structure changes of rigid composite electrodes containing multilayered Ti$_3$C$_2$T$_x$ particles (Figure 3d). However, gravimetric information can be obtained only for rigid and thin coatings. In such layers, the profiles of the acoustic waves generated by the quartz crystal sensor oscillations remain constant across the coated films (as seen in Figure 6d). In contrast, thick viscoelastic films vibrate with a different velocity than the quartz crystal surface, decaying across the film's thickness, that is, the oscillation energy dissipates (see the sloppy velocity profiles in Figure 6d, more explanation about this gravimetric and non-gravimetric EQCM-D measurements for the characterization of electrode materials can be found in refs. [49,63]). Acoustic response resulting from the interaction of acoustic waves with viscoelastic materials is specific for each overtone order, n, and measurements of the resonance frequency and the related dissipation factors for at least 3 overtone orders allow quantification of viscoelastic properties of the electrodes. The measured quantities for each n are simultaneously fitted to a suitable viscoelastic model to extract the complex shear modulus of the electrode, that is, its shear storage (elastic) modulus, G', and shear loss modulus, G'' (linked to the shear viscosity, η).

Application of EQCM-D measurements to acoustically thick MXene coatings (470 nm thick film) immersed in 1 M Li$_2$SO$_4$ solution revealed pronounced changes in their viscoelastic properties as a function of the applied potential.[64] The characteristic pattern of the intercalation-induced changes of $\Delta f/n$ and ΔD (called herein "viscoelastic signature" in terms of EQCM-D methodology) recorded during 100 cycles is shown in Figure 6d. A magnified EQCM-D response for 3 selected cycles is shown on the right panels. As can be seen, the acoustic waves generated on the higher overtone orders with their smaller penetration depth, d, compared to that for the lower overtones show
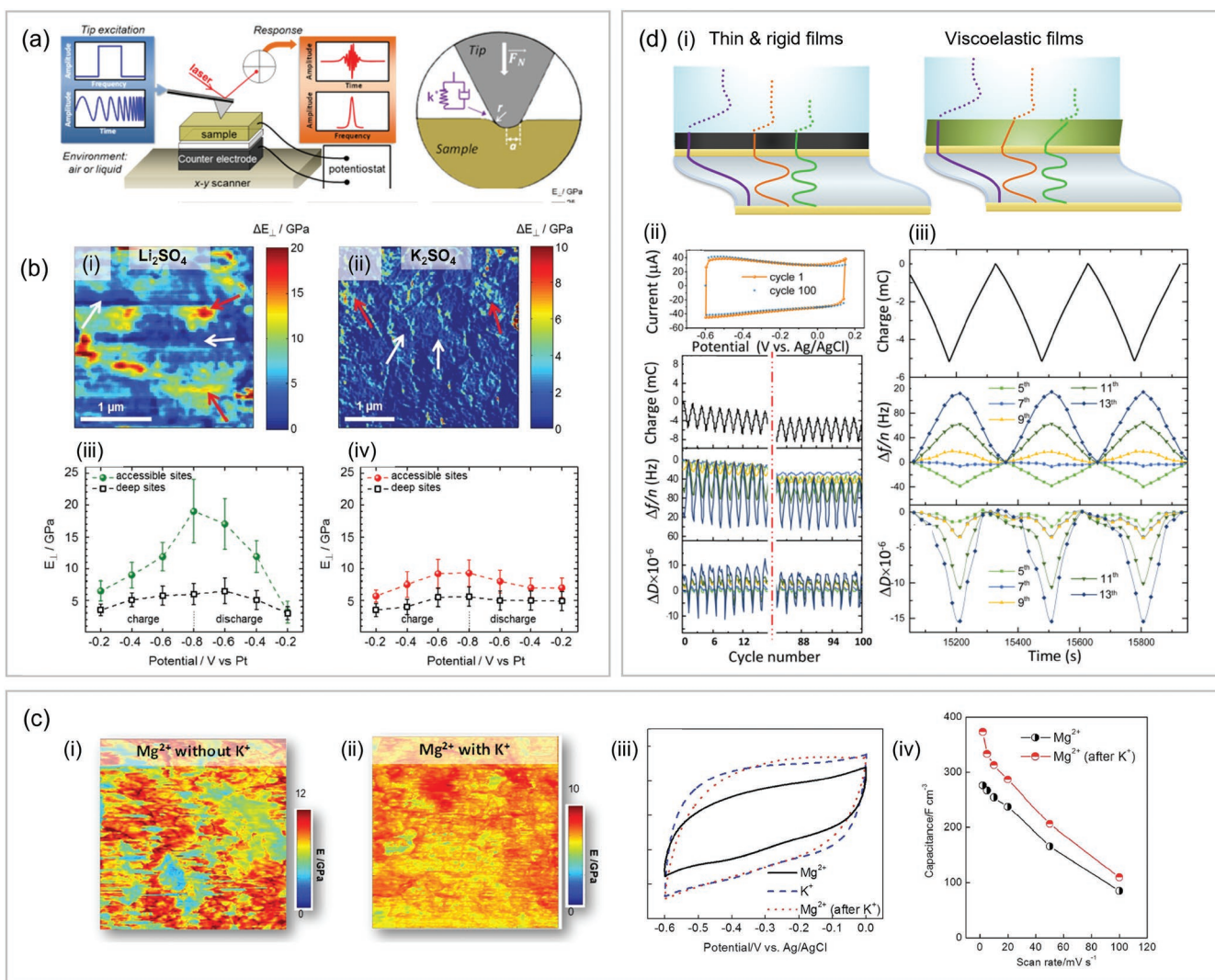
Figure 6. In situ monitoring of mechanical changes in $Ti_3C_2T_x$ electrodes a) Schematic representation of the experimental setup, where the AFM tip vibrates in contact with the sample's surface with a band excitation waveform. b) Elastic modulus mapping of negatively charged (−0.8 V) MXene films immersed in i) Li_2SO_4 ii) K_2SO_4 electrolytes. Based on the maximal variations in the elastic modulus one can identify the shallow and the deep intercalation sites in the MXene electrodes for both Li^+ and K^+ ions insertion (panels (iii) and (iv) respectively). Reproduced with permission.[56] Copyright 2016, Wiley. c) The variations in the elastic modulus of $Ti_3C_2T_x$ after insertion of Mg^{2+} ions (i) and after pre-cycling in K_2SO_4 solutions. (ii). The corresponding changes in the CVs and the rate capability are presented in (iii) and (iv). Reproduced with permission.[43] Copyright 2017, The Royal Society of Chemistry d) i) Schematic descriptions of acoustic wave velocity profiles generated across the quartz crystal, loaded by acoustically thin and thick (viscoelastic) films. ii) CVs, frequency, and dissipation of thick MXene films throughout 100 cycles iii) An enlarged view of the charge frequency and dissipation changes recorded during 3 cycles. Reproduced with permission.[65] Copyright 2017, American Chemical Society.

a spectacular increase in the resonance frequency and the corresponding decrease in the dissipation factor during Li^+ ions intercalation. Fitting the experimental data to a Voight-type viscoelastic model reveals that the insertion of Li^+ ions results in the stiffening of the MXene electrodes. During the reverse process (i.e., in the course of extraction of Li^+ ions), the electrodes demonstrate softening returning to the initial viscoelastic state of the completely deintercalated state of the MXene electrodes. Further, it was shown that the intrinsic rate of the intercalation-induced stiffening/softening of the electrodes is high as the amplitude of the potential-dependent $\Delta f/n$ and ΔD changes, does not depend on the scan rate ranging from 20 to 100 mV s^{-1}.[64] The stiffening of MXene structures upon ions

insertion is in line with the previously presented AFM results which have demonstrated similar behavior (Figure 6b).

An interesting application of the Mxenes' viscoelastic character is the structural engineering of composite battery electrodes. Considering the high flexibility of MXenes, and the strong electrostatic interactions between their layers, new types of hybridized battery-supercapacitor electrodes have been proposed. Such electrodes exhibit improved energy and power density performance. They may provide high specific gravimetric capacity since electrochemically inactive polymer binders can be replaced by supercapacitive MXene particles. They also provide enhanced rate capability due to the high electronic conductivity of Mxenes.[66–68]

8. Conclusion and Perspectives

The main focus of this review was on the unique redox properties of Mxenes, a new class of 2D materials for use in the field of energy storage and conversion, which interact very well with a wide variety of electrolyte solutions including neutral and acidic aqueous solutions, water-in-salt electrolytes, ionic liquids, and organic electrolyte solutions. Our approach was based on the idea that to consider MXenes as good active mass candidates for practical batteries and supercapacitors electrodes, they should be carefully characterized by a variety of electrochemical and in situ structure-sensitive techniques with sufficiently different spatial and time resolutions. Application of the classical electroanalytical techniques (such as CV, chronopotentiometry, various current and potential pulsed techniques, impedance spectroscopy, etc.) provide averaged electrochemical characteristics on the scale of entire electrodes which can be complemented by the data obtained simultaneously (or in parallel) using a number of local structure-sensitive techniques (e.g., in situ AFM, Fourier transform infrared (FTIR), Raman spectroscopy, etc.). Such a combination of techniques reflects electrode behavior on different scales, which is usually sufficient to understand the character of the charging mechanism of the electrodes. In this regard, efforts should be devoted to the in situ electrochemical investigations of MXenes' structure at the single flakes scale. Being the very basic building block of bulk electrodes, such studies will provide highly valuable information about the intrinsic characteristics of the MXene.[69] As the multilayer arrangement of the MXene electrodes has a determinantal influence on its electrochemical behavior and other potential-induced phenomena, analysis at the single-layer level will significantly expand our understanding of the MXenes' nature and facilitate the further enhancement of its charge storage capabilities.

Table 1 summarizes the main techniques for in situ characterization of MXene electrodes. These methods are highly relevant for further investigations of new MXene compounds which like $Ti_3C_2T_x$ possess pseudocapacitive nature response due to their rich surface chemistry. Yet, despite the similarities in the surface composition and the layer structure of different MXene compounds, they may exhibit pronounced differences in their electrochemical performance. As the charging mechanism of

Table 1. Relevant in situ techniques for characterization of MXene structures.

Provided information	In situ techniques	Relevant application to MXene research	Main limitations	Representing studies
Gravimetric information	EQCM	Monitoring of ions and solvent molecules fluxes, formation of surface films	Can be applied only on acoustically thin films with sufficient rigidity	[23,35,48,70]
Morphological variations	Dilatometry	Assessment of expansion/shrinkage of MXene electrodes	Limited to changes in the Z- direction	[56]
	AFM	Tracking of variations MXene morphology on a nanometric scale	Provide only local information (usually limited to several micrometers)	[42,43,60]
	SEM[a]	Changes in the electrodes' morphology Formation of surface films, dendrite growth	Only low vapor-pressure electrolytes can be applied	
	EQCM-D	Monitoring of porous structure and thickness of MXene electrodes	Can be applied only on acoustically thin films with sufficient rigidity. Necessitates the use of complex hydrodynamic modeling	[49]
Structural changes	X-ray diffraction	Atomic scale changes in the unit cell parameters of operated MXene structures	Fail to capture local heterogeneities on the microstructural level	[55,56]
	TEM[a]	Phase transformations, lattice expansion/contraction at nanoscale resolution	Only low vapor-pressure electrolytes can be applied, provide only local information	
	Raman spectroscopy	Localized variation of MXene surface terminations	Potential signal noise from liquid electrolytes	[32]
	FTIR spectroscopy[a]	Localized variation of MXene surface terminations	Potential signal noise from liquid electrolytes	
	UV–vis	Changes in the oxidation state of the metallic elements	Difficult to correlate the charge Q and the change of the plasmonic peaks	[52,71]
	XANES	Changes in the oxidation state of the metallic elements	Measurements with a high signal-to-noise ratio require a strong X-ray source synchrotron	[30,52]
	EXAFS	Local structural changes, bond length changes	Can only provide the macroscopic view (average) of changes	[52]
Mechanical properties	EQCM-D	Variations in the viscoelastic properties of MXene electrodes	Interpretation of the signals and the implementation of viscoelastic modeling might be challenging.	[72]
	AFM	Local changes in the elastic modulus of the MXene electrodes	Local rather macroscopic characterization of the mechanical properties	[65]

[a]The methods marked have not yet been reported for studies of MXene electrodes.

**ADVANCED
SCIENCE NEWS**

www.advancedsciencenews.com

**ADVANCED
ENERGY
MATERIALS**

www.advenergymat.de

many new MXene types moieties (such as vanadium, molybdenum, or niobium-based MXene) is not well explored so far, the use of the following in situ techniques are essential to get deeper insights into their electrochemical behavior.

Given the findings presented, it appears that the charging process of $Ti_3C_2T_x$ electrodes in aqueous acidic solutions was adequately addressed. Nevertheless, additional research is needed to understand the behavior of MXenes electrodes in other environments. In our view particular attention should be paid to the following systems:

MXene electrodes in neutral aqueous solutions: The above contradiction between the low surface capacity of the Ti_3C_2Tx electrodes and their high specific capacity values should be further explored by sensitive in situ techniques. A possible explanation for this question was provided by ex situ Ti K-edge XAS spectroscopy which showed slight changes in the Ti oxidation state by $0.05\overline{e}$ upon application of negative potentials (−0.05 to −0.45 V vs Ag/AgCl) in 1 M Li_2SO_4. This small change in the titanium atoms' oxidation state, corresponds well to the extra charge measured for these systems, ≈20 mAh g^{-1}.[19] Consequently, MXenes cannot be considered as an active mass in double-layer capacitors, but rather as an active mass whose behavior is pseudocapacitive. In this aspect, the charging process of MXene electrodes is somewhat similar to that of MnO_2 electrodes in aqueous solutions which also exhibit rectangular-shaped pseudocapacitive response.[73] Further clarification of this issue may be achieved by using sensitive in situ techniques, particularly XAS, advanced UV–vis, FTIR, and in situ Raman spectroscopies in conjunction with electrochemical tools, and single studies. Such studies can set guidelines on how to read properly the electrodes' response by the various analytical techniques. For instance, how shifts in Raman peaks reflect changes in the oxidation state of major atoms and how these correlate to changes in the steady state of the electrodes' specific capacity. The influence of surface chemistry on the performance of MXene electrodes in aqueous and non-aqueous solutions should be further explored. MXenes are conventionally synthesized in HF-containing solutions, which results in F-rich surface chemistry (In addition to O- and OH- terminations[7]). In trying to avoid the use of hazardous HF, alternative fluorine-free synthesis methods have recently been proposed.[74,75] These alternative synthesis approaches result in the formation of MXene electrodes with new surface chemistries and most probably, modified structural features (such as the electrodes' wettability, hierarchical porous structure, etc.) which may have a significant influence on their charging mechanism, and at the same time on their cycling performance.

Additional research efforts should be devoted to the influence of the pre-insertion of cations on the performance of MXene electrodes. As previously indicated, the pre-insertion of K$^+$ ions prior to operation in Mg salt solutions (in which Mg ions insertion/deinsertion is the major electrochemical process) substantially improves the specific capacity and rate capability of MXenes electrodes. However, the effect of the cations' characteristics, particularly their size-to-charge ratio, on the performance of MXenes electrodes which undergo red-ox processes which involve cations insertion/de-insertion cycling should be further studied. Suitable in situ techniques for addressing these issues are EQCM-D, XRD, and AFM (preferentially should be applied in parallel, in single studies, to the same systems). In situ investigations of $Ti_3C_2T_x$ in aqueous solutions comprising Al^{3+} and transition metal ions (especially Zn^{2+}) are highly desirable. Finally, the recent growing interest in Zn batteries brings new opportunities for the utilization of MXenes as an active mass in electrodes for Zn ions insertion and Zn deposition.[76,77] In this regard, the effect of the MXenes' surface chemistry and morphology on the performance of possible Zn deposition process is very interesting and deserves research work, for which the use of the above-described in situ analytical tools can contribute a lot.

MXenes in highly concentrated aqueous electrolyte solutions: As the concept of "water in salt" electrolytes are relatively new, additional research efforts should be conducted to decipher the charging mechanisms of MXene electrodes in these electrolyte solutions. Of particular interest is the influence of the concentrated electrolytes comprising various mono and multivalent ions on the MXenes structure during reversible ions insertion/deinsertion processes. Working with concentrated LiCl or LiBr results in a significant widening of both the positive and negative zones, as demonstrated. However, while the increased cathodic stability can be attributed to the inhibition of H_2 evolution, the origin of the expanded anodic stability remained unclear. Furthermore, as shown, some MXene electrodes exhibit redox behavior when positive potentials are applied, whilst others present a rectangular/capacitive type voltammetric response in the same electrolyte systems. It is interesting to understand the mechanism of such red-ox behavior and the origin of the peaks in the voltammetric response of these electrodes. In addition, some WIS electrolytes (TFSI-based electrolytes for example) induce the formation of passivation layers upon negative polarization. The application of in situ methods including EQCM-D, AFM, and Raman spectroscopy (in the same studies, in conjunction with electrochemical tools) can provide valuable information about the real-time formation of these layers and their effects on the performance of MXene electrodes. Last, information about the influence of highly concentrated electrolytes on the mechanical properties of MXenes will be highly valuable. The above-proposed studies are not important just for the practical field of energy storage and conversion. They will enrich the playground of very basic electro-analytical chemistry and spectro-electrochemistry.

MXene electrodes in nonaqueous electrolyte systems: Generally speaking, conducting in situ experiments in aqueous solutions (either neutral or acidic) are significantly simpler than similar studies in non-aqueous solutions. Organic and ionic liquids electrolyte solutions are highly sensitive to the presence of humidity, and even traces of water can severely affect the results and their significance. Considering the fact that many instruments cannot be placed into glove boxes or kept under an inert atmosphere, special attempts should be made to make toward the development of properly sealed cells. Furthermore, the formation of solid electrolyte interphases on electrodes in many organic electrolyte solutions (especially at low potentials) may cause severe difficulties in interpreting the obtained data. This becomes even more challenging in measurements of thin electrode films when the ratio between the electrolyte solution's mass and the active electrode's mass is substantially large.[78] As a result, relatively few in situ studies (compare to

ADVANCED
SCIENCE NEWS
www.advancedsciencenews.com

ADVANCED
ENERGY
MATERIALS
www.advenergymat.de

aqueous solutions) were conducted so far on MXene electrodes in aprotic solutions.

The recent developments in the utilization of electron microscopies for in situ measurements of electrode materials[79,80] open research new capabilities for MXenes' studies as well. These methods enable real-time monitoring of electrodes that operate in low vapor-pressure electrolytes (such as ionic liquids). The use of high-resolution scanning electron microscopy (SEM) may provide desirable information about potentially induced morphological changes occurring in operated MXene electrodes. Considering the recent advances in the use of MXenes as an effective current collector for metal plating,[81,82] the use of in situ SEM can significantly promote the understanding of the nucleation process and formation of dendrites on MXene surfaces. in situ transmission electron microscopy (TEM) analysis can shed a light on structural evolutions such as phase transformation or crystal expansion of the MXene structures upon application of potential. Such insights are critically important to understand the degradation phenomena of MXene electrodes an issue that is not often discussed in published studies.

Targeting practical implementation of MXenes as anodes in non-aqueous rechargeable batteries beyond Li-ion batteries (particularly for K and Na ion battery systems for large energy storage), further in situ experiments related to the effect of the electrolyte solutions on the MXenes' charging mechanisms and the structural/mechanical associated phenomena should be carried out.

Nano-confined electrolytes molecules in MXene electrodes: Regardless of the selected electrolytic environment, special attention should be focused on the contribution of the co-inserted solvent molecules to the charging mechanisms of MXenes. Unlike the majority of conventional batteries and supercapacitors electrodes, MXenes belong to a special class of hydrophilic electrodes containing intrinsically solvent molecules presenting in their interspaces. The amount of co-inserted solvent molecules (AKA confined electrolyte solutions) depends strongly on the amount of the inserted electrolytic cations, the type of the solvent, and the porosity/morphology of the $Ti_3C_2T_x$ moieties. In this respect, MXenes resemble the class of electronically conducting polymers. By this property, MXenes are also similar to the class of nanoporous carbon electrodes, however, differing from them by the exclusive insertion of the cations rather than both cations and anions during their charging/discharging. Neutron-related techniques have been used ex situ to observe the status of included solvent molecules between the MXenes interlayer spacing. For example, inelastic neutron scattering was used to analyze the vibrational states of the interfacial H_2O molecule and neutron backscattering is capable to reveal the confinement of organic solvents.[29,82] A straightforward way to quantify the amount of co-inserted/co-extracted solvent molecules during electrodes' charge-discharge processes is to supplement the use of the above-mentioned combination of analytical techniques by application of EQCM-D in its gravimetric mode (the use of conventional QCM without dissipation monitoring is insufficient for a thorough quantitative analysis). In this way, the dynamics of the cations-solvent molecules' competition for the occupation of the sites in the confined MXene interlayer spaces can be quantitatively studied

and further compared with the related molecular dynamics calculations. Such studies, beyond their importance for the field of non-aqueous rechargeable batteries, will mark a frontier in analytical chemistry.

Conflict of Interest

The authors declare no conflict of interest.

[1] V. Augustyn, P. Simon, B. Dunn, *Energy Environ. Sci.* **2014**, *7*, 1597.

[2] Y. Liu, S. P. Jiang, Z. Shao, *Intercalation pseudocapacitance in electrochemical energy storage: recent advances in fundamental understanding and materials development*, Elsevier, UK **2020**.

[3] S. M. Bak, R. Qiao, W. Yang, S. Lee, X. Yu, B. Anasori, H. Lee, Y. Gogotsi, X. Q. Yang, *Adv. Energy Mater.* **2017**, *7*, 1700358.

[4] R. Liu, W. Cao, D. Han, Y. Mo, H. Zeng, H. Yang, W. Li, *J. Alloys Compd.* **2019**, *793*, 505.

[5] J. Halim, S. Kota, M. R. Lukatskaya, M. Naguib, M. Q. Zhao, E. J. Moon, J. Pitock, J. Nanda, S. J. May, Y. Gogotsi, M. W. Barsoum, *Adv. Funct. Mater.* **2016**, *26*, 3118.

[6] Q. Wan, S. Li, J. B. Liu, *ACS Appl. Mater. Interfaces* **2018**, *10*, 6369.

[7] H. Huang, X. Chu, Y. Xie, B. Zhang, Z. Wang, Z. Duan, N. Chen, Z. Xu, H. Zhang, W. Yang, *ACS Nano* **2022**, *16*, 3776.

[8] S. Venkateshalu, A. N. Grace, *MXenes—A new class of 2D layered materials: Synthesis, properties, applications as supercapacitor electrode and beyond*, Elsevier, UK **2020**.

[9] M. Naguib, R. R. Unocic, B. L. Armstrong, J. Nanda, *Dalton Trans.* **2015**, *44*, 9353.

[10] A. Lipatov, M. Alhabeb, M. R. Lukatskaya, A. Boson, Y. Gogotsi, A. Sinitskii, *Adv. Electron. Mater.* **2016**, *2*, 1600255.

[11] M. Alhabeb, K. Maleski, B. Anasori, P. Lelyukh, L. Clark, S. Sin, Y. Gogotsi, *Chem. Mater.* **2017**, *29*, 7633.

[12] R. M. Ronchi, J. T. Arantes, S. F. Santos, *Synthesis, structure, properties and applications of MXenes: Current status and perspectives*, Elsevier, UK **2019**.

[13] Y. Gogotsi, B. Anasori, *ACS Nano* **2019**, *13*, 8491.

[14] A. Champagne, J.-C. Charlier, *JPhys Mater.* **2020**, *3*, 3.

[15] B. Anasori, M. R. Lukatskaya, Y. Gogotsi, *Nat. Rev. Mater.* **2017**, *2*, 16098.

[16] B. M. Jun, S. Kim, J. Heo, C. M. Park, N. Her, M. Jang, Y. Huang, J. Han, Y. Yoon, *Review of MXenes as new nanomaterials for energy storage/delivery and selected environmental applications*, Springer, Berlin **2019**.

[17] D. Liu, Z. Shadike, R. Lin, K. Qian, H. Li, K. Li, S. Wang, Q. Yu, M. Liu, S. Ganapathy, X. Qin, Q. H. Yang, M. Wagemaker, F. Kang,

X. Q. Yang, B. Li, *Review of Recent Development of In Situ/Operando Characterization Techniques for Lithium Battery Research*, Wiley-VCH, Weinheim **2019**.

[18] X. Su, J. Ye, Y. Zhu, *Advances in in-situ characterizations of electrode materials for better supercapacitors*, Vol. *54*, Elsevier, UK **2021**, pp. 242–253.

[19] M. Okubo, A. Sugahara, S. Kajiyama, A. Yamada, *Acc. Chem. Res.* **2018**, *51*, 591.

[20] J. Nan, X. Guo, J. Xiao, X. Li, W. Chen, W. Wu, H. Liu, Y. Wang, M. Wu, G. Wang, J. Nan, J. Xiao, X. Li, H. Liu, Y. Wang, M. Wu, X. Guo, G. X. Wang, W. Chen, W. Wu, *Small* **2021**, *17*, 1902085.

[21] F. Malchik, N. Shpigel, M. D. Levi, T. S. Mathis, A. Mor, Y. Gogotsi, D. Aurbach, *J. Mater. Chem. A* **2019**, *7*, 19761.

[22] F. Malchik, N. Shpigel, M. D. Levi, T. S. Mathis, A. Mor, Y. Gogotsi, D. Aurbach, *J. Mater. Chem. A* **2019**, *7*, 19761.

[23] N. Shpigel, A. Chakraborty, F. Malchik, G. Bergman, A. Nimkar, B. Gavriel, M. Turgeman, C. N. Hong, M. R. Lukatskaya, M. D. Levi, Y. Gogotsi, D. T. Major, D. Aurbach, *J. Am. Chem. Soc.* **2021**, *143*, 12552.

[24] X. Wang, T. S. Mathis, Y. Sun, W.-Y. Tsai, N. Shpigel, H. Shao, D. Zhang, K. Hantanasirisakul, F. Malchik, N. Balke, D. Jiang, P. Simon, Y. Gogotsi, *ACS Nano* **2021**, *15*, 15274.

[25] X. Tian, Q. Zhu, B. Xu, *ChemSusChem* **2021**, *14*, 2501.

[26] X. Mu, D. Wang, F. Du, G. Chen, C. Wang, Y. Wei, Y. Gogotsi, Y. Gao, Y. Dall'Agnese, *Adv. Funct. Mater.* **2019**, *29*, 1902953.

[27] M. R. Lukatskaya, S. Kota, Z. Lin, M.-Q. Zhao, N. Shpigel, M. D. Levi, J. Halim, P.-L. Taberna, M. W. Barsoum, P. Simon, Y. Gogotsi, *Nat. Energy* **2017**, *2*, 17105.

[28] C. Zhan, M. Naguib, M. Lukatskaya, P. R. C. Kent, Y. Gogotsi, D. Jiang, *J. Phys. Chem. Lett.* **2018**, *9*, 1223.

[29] X. Wang, T. S. Mathis, K. Li, Z. Lin, L. Vlcek, T. Torita, N. C. Osti, C. Hatter, P. Urbankowski, A. Sarycheva, M. Tyagi, E. Mamontov, P. Simon, Y. Gogotsi, *Nat. Energy* **2019**, *2*, 228.

[30] M. R. Lukatskaya, S.-M. Bak, X. Yu, X.-Q. Yang, M. W. Barsoum, Y. Gogotsi, *Adv. Energy Mater.* **2015**, *5*, 1500589.

[31] H. Shao, K. Xu, Y.-C. Wu, A. Iadecola, L. Liu, H. Ma, L. Qu, E. Raymundo-Piñero, J. Zhu, Z. Lin, P.-L. Taberna, P. Simon, *ACS Energy Lett.* **2020**, *5*, 2873.

[32] D. Johnson, K. Hansen, R. Yoo, A. Djire, *ChemElectroChem* **2022**, *9*, 202200555.

[33] M. Hu, Z. Li, T. Hu, S. Zhu, C. Zhang, X. Wang, *ACS Nano* **2016**, *10*, 11344.

[34] X. Mu, D. Wang, F. Du, G. Chen, C. Wang, Y. Wei, Y. Gogotsi, Y. Gao, Y. Dall'Agnese, *Adv. Funct. Mater.* **2019**, *29*, 1902953.

[35] K. Zheng, Y. Xian, Z. Lin, *Adv. Mater. Interfaces* **2022**, *9*, 2200112.

[36] A. Borenstein, O. Hanna, R. Attias, S. Luski, T. Brousse, D. Aurbach, *Carbon-based composite materials for supercapacitor electrodes: A review*, Vol. *5*, Royal Society of Chemistry, London **2017**, pp. 12653–12672.

[37] Z. Li, D. Guo, Y. Liu, H. Wang, L. Wang, *Chem. Eng. J.* **2020**, *397*, 125418.

[38] A. Saha, N. Shpigel, Rosy, N. Leifer, S. Taragin, T. Sharabani, H. Aviv, I. Perelshtein, G. D. Nessim, M. Noked, Y. Gogotsi, *Adv. Funct. Mater.* **2021**, *31*, 2106294.

[39] M. Naguib, J. Come, B. Dyatkin, V. Presser, P.-L. Taberna, P. Simon, M. W. Barsoum, Y. Gogotsi, *Electrochem. Commun.* **2012**, *16*, 61.

[40] M. Ghidiu, J. Halim, S. Kota, D. Bish, Y. Gogotsi, M. W. Barsoum, *Chem. Mater.* **2016**, *28*, 3507.

[41] M. R. Lukatskaya, O. Mashtalir, C. E. Ren, Y. Dall'Agnese, P. Rozier, P. L. Taberna, M. Naguib, P. Simon, M. W. Barsoum, Y. Gogotsi, *Science* **2013**, *341*, 1502.

[42] J. Come, J. M. Black, M. R. Lukatskaya, M. Naguib, M. Beidaghi, A. J. Rondinone, S. V. Kalinin, D. J. Wesolowski, Y. Gogotsi, N. Balke, *Nano Energy* **2015**, *17*, 27.

[43] Q. Gao, J. Come, M. Naguib, S. Jesse, Y. Gogotsi, N. Balke, *Faraday Discuss.* **2017**, *199*, 393.

[44] N. Shpigel, M. D. Levi, S. Sigalov, T. S. Mathis, Y. Gogotsi, D. Aurbach, *J. Am. Chem. Soc.* **2018**, *140*, 8910.

[45] Q. Gao, W. Sun, P. Ilani-Kashkouli, A. Tselev, P. R. C. Kent, N. Kabengi, M. Naguib, M. Alhabeb, W. Y. Tsai, A. P. Baddorf, J. Huang, S. Jesse, Y. Gogotsi, N. Balke, *Energy Environ. Sci.* **2020**, *13*, 2549.

[46] M. D. Levi, M. R. Lukatskaya, S. Sigalov, M. Beidaghi, N. Shpigel, L. Daikhin, D. Aurbach, M. W. Barsoum, Y. Gogotsi, *Adv. Energy Mater.* **2014**, *5*, 1400815.

[47] N. Shpigel, M. D. Levi, S. Sigalov, L. Daikhin, D. Aurbach, *Acc. Chem. Res.* **2018**, *51*, 69.

[48] N. Shpigel, M. D. Levi, S. Sigalov, T. S. Mathis, Y. Gogotsi, D. Aurbach, *J. Am. Chem. Soc.* **2018**, *140*, 8910.

[49] M. D. Levi, M. R. Lukatskaya, S. Sigalov, M. Beidaghi, N. Shpigel, L. Daikhin, D. Aurbach, M. W. Barsoum, Y. Gogotsi, *Adv. Energy Mater.* **2015**, *5*, 1400815.

[50] X. Wang, T. S. Mathis, Y. Sun, W.-Y. Tsai, N. Shpigel, H. Shao, D. Zhang, K. Hantanasirisakul, F. Malchik, N. Balke, D. Jiang, P. Simon, Y. Gogotsi, *ACS Nano* **2021**, *15*, 15274.

[51] P. Salles, E. Quain, N. Kurra, A. Sarycheva, Y. Gogotsi, *Small* **2018**, *14*, 1802864.

[52] X. Wang, S. M. Bak, M. Han, C. E. Shuck, C. McHugh, K. Li, J. Li, J. Tang, Y. Gogotsi, *ACS Energy Lett.* **2022**, *7*, 30.

[53] G. Ma, H. Shao, J. Xu, Y. Liu, Q. Huang, P. L. Taberna, P. Simon, Z. Lin, *Nat. Commun.* **2021**, *12*, 5085.

[54] Y. Li, H. Shao, Z. Lin, J. Lu, L. Liu, B. Duployer, P. O. Å. Persson, P. Eklund, L. Hultman, M. Li, K. Chen, X. H. Zha, S. Du, P. Rozier, Z. Chai, E. Raymundo-Piñero, P. L. Taberna, P. Simon, Q. Huang, *Nat. Mater.* **2020**, *19*, 894.

[55] Z. Lin, P. Rozier, B. Duployer, P.-L. Taberna, B. Anasori, Y. Gogotsi, P. Simon, *Electrochem. Commun.* **2016**, *72*, 50.

[56] N. Jäckel, B. Krüner, K. L. van Aken, M. Alhabeb, B. Anasori, F. Kaasik, Y. Gogotsi, V. Presser, *ACS Appl. Mater. Interfaces* **2016**, *8*, 32089.

[57] A. Lipatov, H. Lu, M. Alhabeb, B. Anasori, A. Gruverman, Y. Gogotsi, A. Sinitskii, *Sci. Adv.* **2018**, *4*, aat0491.

[58] J. Zhang, N. Kong, S. Uzun, A. Levitt, S. Seyedin, P. A. Lynch, S. Qin, M. Han, W. Yang, J. Liu, X. Wang, Y. Gogotsi, J. M. Razal, *Adv. Mater.* **2020**, *32*, 2001093.

[59] V. H. Nguyen, R. Tabassian, S. Oh, S. Nam, M. Mahato, P. Thangasamy, A. Rajabi-Abhari, W. J. Hwang, A. K. Taseer, I.-K. Oh, *Adv. Funct. Mater.* **2020**, *30*, 1909504.

[60] Q. Gao, W.-Y. Tsai, N. Balke, *Electrochem. Sci. Adv.* **2022**, *2*, e2100038.

[61] M. Kocun, A. Labuda, A. Gannepalli, R. Proksch, *Rev. Sci. Instrum.* **2015**, *86*, 083706.

[62] J. Come, Y. Xie, M. Naguib, S. Jesse, S. V. Kalinin, Y. Gogotsi, P. R. C. Kent, N. Balke, *Adv. Energy Mater.* **2016**, *6*, 1502290.

[63] N. Shpigel, M. D. Levi, D. Aurbach, *Energy Storage Mater.* **2019**, *21*, 399.

[64] N. Shpigel, M. R. Lukatskaya, S. Sigalov, C. E. Ren, P. Nayak, M. D. Levi, L. Daikhin, D. Aurbach, Y. Gogotsi, *ACS Energy Lett.* **2017**, *2*, 1407.

[65] J. Come, Y. Xie, M. Naguib, S. Jesse, S. v. Kalinin, Y. Gogotsi, P. R. C. Kent, N. Balke, *Adv. Energy Mater.* **2016**, *6*, 1502290.

[66] F. Malchik, N. Shpigel, M. D. Levi, T. R. Penki, B. Gavriel, G. Bergman, M. Turgeman, D. Aurbach, Y. Gogotsi, *Nano Energy* **2021**, *79*, 105433.

[67] M. Boota, E. Jung, R. Ahuja, T. Hussain, *J. Mater. Chem. A* **2021**, *9*, 20356.

[68] C. (John) Zhang, S.-H. Park, A. Seral-Ascaso, S. Barwich, N. McEvoy, C. S. Boland, J. N. Coleman, Y. Gogotsi, V. Nicolosi, *Nat. Commun.* **2019**, *10*, 849.

[69] L. Jiang, D. Zhou, J. Yang, S. Zhou, H. Wang, X. Yuan, J. Liang, X. Li, Y. Chen, H. Li, *J. Mater. Chem. A* **2022**, *10*, 13651.

**ADVANCED
SCIENCE NEWS**

www.advancedsciencenews.com

**ADVANCED
ENERGY
MATERIALS**

www.advenergymat.de

[70] Enhanced Performance of Ti$_3$C$_2$T$_x$ (MXene) Electrodes in Concentrated ZnCl$_2$ Solutions: A Combined Electrochemical and EQCM-D Study.

[71] J. Li, X. Wang, W. Sun, K. Maleski, C. E. Shuck, K. Li, P. Urbankowski, K. Hantanasirisakul, X. Wang, P. Kent, H. Wang, Y. Gogotsi, *ChemElectroChem* **2021**, *8*, 151.

[72] N. Shpigel, M. R. Lukatskaya, S. Sigalov, C. E. Ren, P. Nayak, M. D. Levi, L. Daikhin, D. Aurbach, Y. Gogotsi, *In Situ Monitoring of Gravimetric and Viscoelastic Changes in 2D Intercalation Electrodes*, Vol. 2, American Chemical Society, Washington, DC, **2017**, pp. 1407–1415.

[73] M. J. Young, A. M. Holder, S. M. George, C. B. Musgrave, *Chem. Mater.* **2015**, *27*, 1172.

[74] Z. Bao, C. Lu, X. Cao, P. Zhang, L. Yang, H. Zhang, D. Sha, W. He, W. Zhang, L. Pan, Z. Sun, *Chin. Chem. Lett.* **2021**, *32*, 2648.

[75] T. Su, X. Ma, J. Tong, H. Ji, Z. Qin, Z. Wu, *J. Mater. Chem. A* **2022**, *10*, 10265.

[76] Y. Tian, Y. An, C. Wei, B. Xi, S. Xiong, J. Feng, Y. Qian, *ACS Nano* **2019**, *13*, 11676.

[77] B. Gavriel, N. Shpigel, F. Malchik, G. Bergman, M. Turgeman, M. D. Levi, D. Aurbach, *Energy Storage Mater.* **2021**, *38*, 535.

[78] V. Dargel, N. Shpigel, S. Sigalov, P. Nayak, M. D. Levi, L. Daikhin, D. Aurbach, *Nat. Commun.* **2017**, *8*, 1389.

[79] C. Zhang, K. L. Firestein, J. F. S Fernando, D. Siriwardena, J. E. von Treifeldt, D. Golberg, C. Zhang, K. L. Firestein, J. F. S Fernando, D. Siriwardena, J. E. von Treifeldt, D. Golberg, *Adv. Mater.* **2020**, *32*, 1904094.

[80] Y. Li, X. Cheng, Y. Zhang, K. Zhao, *Mater. Today Nano* **2019**, *7*, 100040.

[81] C. Wei, Y. Tao, Y. An, Y. Tian, Y. Zhang, J. Feng, Y. Qian, C. L. Wei, Y. Tao, Y. L. An, Y. Tian, Y. C. Zhang, J. K. Feng, Y. T. Qian, *Adv. Funct. Mater.* **2020**, *30*, 2004613.

[82] N. C. Osti, M. Naguib, K. Ganeshan, Y. K. Shin, A. Ostadhossein, A. C. T. Van Duin, Y. Cheng, L. L. Daemen, Y. Gogotsi, E. Mamontov, A. I. Kolesnikov, *Phys. Rev. Mater.* **2017**, *1*, 065406.

Gil Bergman was granted an M.Sc. degree in 2021 under the supervision of Prof. Doron Aurbach. He continued his Ph.D. studies in Prof. Aurbach's group and currently focusing on the research and development of aqueous batteries for large energy storage applications and the characterization of electrodes by EQCM-D.

Elad Ballas is an M.SC student in the chemistry department at Bar Ilan University, working under Prof. Doron Aurbach's supervision. His current study focuses on research and development of advanced aqueous electrochemical systems for energy storage applications.

Qiang Gao is a R&D new capabilities team leader at Owens Corning. He obtained Ph.D. in Chemistry at Universite D' Orléans & French National Center for Scientific Research. He held a researcher position at the Max Planck Institute for Chemical Energy Conversion, Oak Ridge National Laboratory, as well as the University of Wisconsin-Madison. His research interests include materials and electrolytes for advanced energy storage and conversion, and in operando spectroscopy and microscopy in quantifying & imaging electrochemical interfaces and pore-scale fluid-solid interactions. He has published over 40 research articles with 2778 Google Scholar citations and H-index 23.

Amey Nimkar obtained his Ph.D. in Chemistry under the supervision of Prof. Ramana from University of Mumbai, India. Later he joined the research group of Prof. Shmaryahu Hoz at Bar Ilan University, Israel. Currently, he is doing Post Doctorate research with Prof. Doron Aurbach at Bar Ilan University, Israel, in the field of rechargeable batteries. His research focuses on development of large energy storage, aqueous mono, and multivalent ion batteries, and organic electrode materials.

Bar Gavriel received his M.Sc. and Ph.D. in Chemistry from Bar Ilan University. Supervised by Prof. Doron Aurbach. Bar's Ph.D. studies were devoted to the development of novel electrochemical systems in aqueous electrolyte solutions.

Mikhael D. Levi is a Professor at Bar-Ilan University working in the lab headed by Prof. D. Aurbach. He received his Ph.D. in 1976 under the supervision of Academician Professor A.N. Frumkin in Moscow State University. He specializes in the development of fine electroanalytical methods for characterization of battery materials. Since 2009, he has been developing a nongravimetric EQCM method adjusted for simultaneous tracking of gravimetric, viscoelastic, and porous structure changes in battery materials.

Daniel Sharon is a senior lecturer of chemistry at the Institute of Chemistry and the Center for Nanoscience and Nanotechnology at the Hebrew University of Jerusalem. (batteries). He received his B.S. degree in chemistry (2010) and his Ph.D. degree (2016) in electrochemistry studying intercalation compounds for Li-ion batteries from Bar-Ilan University, Ramat Gan, Israel. Sharon specializes in the development and study of nanomaterials for electrochemical energy storage applications.

Fyodor Malchik is an associate professor at al-Farabi Kazakh National University. He is head of the Laboratory of electrochemical productions postdoctoral. He received his Ph.D. in 2018 and then was a postdoctoral fellow at Bar-Ilan University from 2018 to 2021. He specializes in the synthesis and development of new intercalation materials for aqueous and non-aqueous batteries and electrolyte transport behavior. In addition, he works on the synthesis, characterization, and application of MXene electrodes for energy storage.


Xuehang Wang is an assistant professor in the Department of Radiation Science and Technology at the Delft University of Technology. She earned her Ph.D. in chemical engineering from the Norwegian University of Science and Technology in 2016 and was a postdoctoral researcher at A.J. Drexel Nanomaterials Institute, Drexel University from 2017 to 2020. Her research focuses on gaining an understanding of the charge mechanisms of energy storage devices, particularly the electrolyte transport at the electrode-electrolyte interfaces of 2D MXenes and various carbon materials.

Netanel Shpigel is a researcher at the Hebrew University of Jerusalem and Bar Ilan University. He completed his Ph.D. in Prof. Doron Auerbach's group and then proceed to post-doctoral studies under the supervision of Prof. Yury Gogotsi (Drexel University) and Prof. Daniel Mandler (the Hebrew University of Jerusalem). He currently focuses on the development of electrochemical microbalance with dissipation monitoring technique (EQCM-D) for in situ monitoring of electrode materials and investigations of aqueous batteries and supercapacitors.

Daniel Mandler is a Professor of Chemistry at the Institute of Chemistry of the Hebrew University. He obtained his education at the Hebrew University and the University of Texas. He served as the Head of the Chemistry School and the Vice Dean for Research of the Faculty of Exact Sciences. He is a visiting principal scientist at the Nanyang Technological University (Singapore). His research interests span from analytical to physical electrochemistry, scanning electrochemical microscopy, conversion, and storage of energy, sol-gel technology, thin films and polymers, forensic science, and nanotechnology. He has supervised more than 75 MSc and 25 Ph.D. students, published 300 papers, and has an h-index of 55.
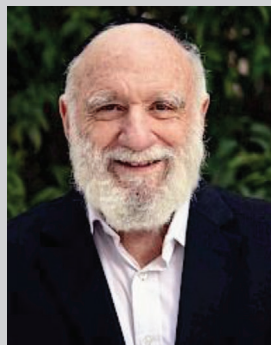
Doron Aurbach is a full professor at the Department of Chemistry, which he chaired during 2001–2005, leading the electrochemistry group (founded in 1985) at Bar Ilan University and the Israel National Research Center for Electrochemical Propulsion (INREP). Professor Aurbach's group studies the electrochemistry of active metals, non-aqueous electrochemistry, intercalation processes, electronically conducting polymers, and water desalination and develops rechargeable batteries and supercapacitors with high energy density including spectroscopic methods for sensitive electrochemical systems. He has published over 720 papers and 30 patents, cited over 92 000 times. He is the technical editor for the Journal of the Electrochemical Society (JES).